

Are your **MRI contrast agents** cost-effective?

Learn more about generic **Gadolinium-Based Contrast Agents**.



**AJNR**

**The Triple Rule-Out for Acute Ischemic Stroke: Imaging the Brain, Carotid Arteries, Aorta, and Heart**

A.D. Furtado, D.D. Adraktas, N. Brasic, S.-C. Cheng, K. Ordovas, W.S. Smith, M.R. Lewin, K. Chun, J.D. Chien, S. Schaeffer and M. Wintermark

This information is current as of April 18, 2024.

*AJNR Am J Neuroradiol* 2010, 31 (7) 1290-1296

doi: <https://doi.org/10.3174/ajnr.A2075>

<http://www.ajnr.org/content/31/7/1290>

**ORIGINAL  
RESEARCH**

A.D. Furtado  
D.D. Adraktas  
N. Brasic  
S.-C. Cheng  
K. Ordovas  
W.S. Smith  
M.R. Lewin  
K. Chun  
J.D. Chien  
S. Schaeffer  
M. Wintermark



# The Triple Rule-Out for Acute Ischemic Stroke: Imaging the Brain, Carotid Arteries, Aorta, and Heart

**BACKGROUND AND PURPOSE:** Ischemic stroke is commonly embolic, either from carotid atherosclerosis or from cardiac origin. These potential sources of emboli need to be investigated to accurately prescribe secondary stroke prevention. Moreover, the mortality in ischemic stroke patients due to ischemic heart disease is greater than that of age-matched controls, thus making evaluation for coronary artery disease important in this patient population. The purpose of this study was to evaluate the image quality of a comprehensive CTA protocol in patients with acute stroke that expands the standard CTA coverage to include all 4 chambers of the heart and the coronary arteries.

**MATERIALS AND METHODS:** One hundred twenty patients consecutively admitted to the emergency department with suspected cerebrovascular ischemia undergoing standard-of-care CTA were prospectively enrolled in our study. We used an original tailored acquisition protocol using a 64-section CT scanner, consisting of a dual-phase intravenous injection of iodinated contrast and saline flush, in conjunction with a dual-phase CT acquisition, ascending from the top of the aortic arch to the vertex of the head, then descending from the top of the aortic arch to the diaphragm. No beta blockers were administered. The image quality, attenuation, and CNRs of the carotid, aortic, vertebral, and coronary arteries were assessed.

**RESULTS:** Carotid, aorta, and vertebral artery image quality was 100% diagnostic (rated good or excellent) in all patients. Coronary artery image quality was diagnostic in 58% of RCA segments, 73% of LAD segments, and 63% of LCX segments. When we considered proximal segments only, the diagnostic quality rose to 71% in the RCA, 83% in the LAD, and 74% in the LCX.

**CONCLUSIONS:** Our stroke protocol achieved excellent opacification of the left heart chambers, the cervical arteries, and each coronary artery, in addition to adequate carotid and coronary artery image quality.

**ABBREVIATIONS:** AP = anteroposterior; BMI = body mass index; CABG = coronary artery bypass graft; CCA = common carotid artery; CNR = contrast-to-noise ratio; CTA = CT angiography; CTDI = CT dose index; ECG = electrocardiogram; ED = emergency department; DLP = dose-length product; 1st Diag = first diagonal branch; HU = Hounsfield unit; ICA = internal carotid artery; LAD = left anterior descending coronary artery; LAV = posterolateral branch originating from the left coronary artery; LCX = left circumflex coronary artery; LM = left main coronary artery; OM = obtuse marginal branch; PDA = posterior descending artery; RCA = right coronary artery; RAV = posterolateral branch originating from the right coronary artery; R-R interval = time between 2 successive R waves; sec = seconds; TEE = transesophageal echocardiography

Patients presenting to the ED with symptoms of acute ischemic stroke are typically imaged by using CT to exclude intracranial hemorrhage and to determine eligibility for intra-

venous thrombolysis. Because the cause of ischemic stroke is commonly embolic, either from carotid atherosclerosis or from the heart,<sup>1</sup> these potential sources of emboli need to be investigated to accurately prescribe secondary stroke prevention. Toward this end, many centers now use a stroke CT protocol that includes CTA of the intracranial and cervical arteries and the aortic arch. This imaging protocol may also include perfusion CT to identify the infarct core and the ischemic penumbra of an acute infarct.<sup>2</sup> To complete the evaluation for potential embolic sources, clinicians often order an additional imaging study, typically a transthoracic or transesophageal echocardiogram.<sup>3,4</sup> This study is typically not conducted in the ED, increasing the time to diagnosis and likely prolonging hospitalization, thereby contributing to an increase in the direct and indirect health care costs. Because CT imaging of the heart is feasible,<sup>5</sup> it would be desirable to image the heart as well during the stroke CT protocol to both expedite this evaluation and reduce the number of additional procedures.

It is also important to evaluate patients with ischemic stroke for coronary artery disease. This evaluation is especially important if the stroke originated from a carotid artery ath-

Received September 7, 2009; accepted after revision January 7, 2010.

From the Departments of Radiology (A.D.F., D.D.A., N.B., K.O., K.C., J.D.C., S.S., M.W.), Epidemiology and Biostatistics (S.-C.C.), Neurology (W.S.S.) and Emergency Medicine (M.R.L.), University of California, San Francisco, San Francisco, California.

This work was supported by the National Center for Research Resources Grant KL2 RR024130 and by a grant from GE Healthcare.

The content of the article is solely the responsibility of the authors and does not necessarily represent the official views of the National Institute of Neurologic Disorders and Stroke, the National Center for Research Resources, the National Institutes of Health, or the other sponsors.

Please address correspondence to Max Wintermark, MD, Neuroradiology Division, Department of Radiology, University of Virginia, PO Box 800170, Charlottesville, VA 22908-0170; e-mail: mw4vh@virginia.edu



Indicates open access to non-subscribers at [www.ajnr.org](http://www.ajnr.org)



Indicates article with supplemental on-line tables.



Indicates article with supplemental online figures

DOI 10.3174/ajnr.A2075

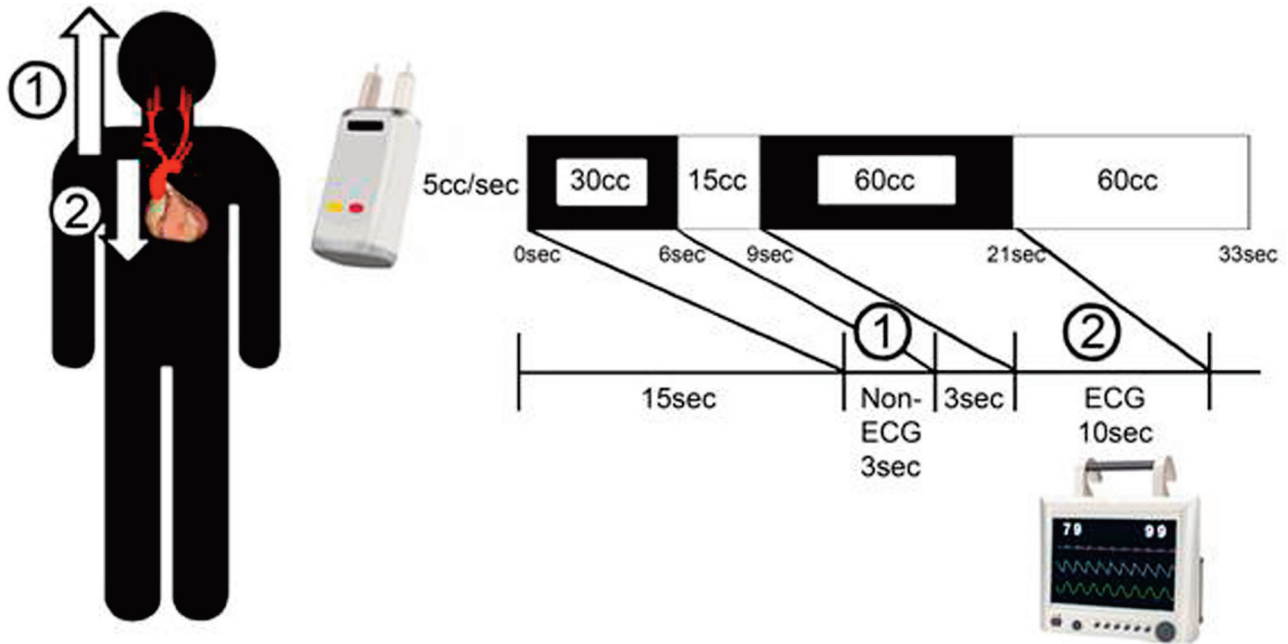


**Fig 1.** Stroke CT protocol design. A bolus of 30 cc of contrast was injected into the right or left cubital vein, followed by a 15 cc saline flush, both at an injection rate of 5 cc per second. The first acquisition (1) (not ECG gated) ascends from the aortic arch origin to the vertex of the head, taking place after a delay determined from perfusion CT used as a bolus test, typically 15 seconds. A second bolus (2) of 60 cc of contrast was injected 3 seconds later and followed by a 60 cc saline flush, again at an injection rate of 5 cc per second. The second acquisition descends from the aortic arch origin to the diaphragm and is ECG gated.

erosclerotic plaque because patients with carotid artery disease are at higher risk for concomitant coronary artery disease than the general population.<sup>6</sup> Indeed, 20%–40% of patients with stroke have abnormal test findings for silent cardiac ischemia.<sup>7–11</sup> Moreover, the mortality rate in patients with cerebrovascular disease due to ischemic heart disease is twice that of age-matched controls.<sup>12–14</sup> Therefore, early diagnosis and treatment of coronary artery disease could improve these patients' quality of life and reduce their mortality. Advances in CT technology have made noninvasive imaging of the coronary arteries possible. Contrast-enhanced CTA with ECG gating permits excellent noninvasive visualization of the coronary arteries when dedicated protocols are used.<sup>15,16</sup>

To allow a comprehensive assessment of patients with acute stroke in 1 radiographic study on admission, we developed a novel stroke CT imaging protocol that includes CTA coverage of the cardiac chambers and the coronary arteries, along with the brain, the aorta, and the carotid arteries. In addition to identifying the location of the infarct, the site of occlusion in the brain, and possible carotid or aortic embolic sources, our protocol evaluates cardiac clots and coronary artery disease. The goal of this study was to assess the image quality afforded by this comprehensive triple rule-out stroke CT imaging study (intracranial and cervical carotid arteries, aorta, and heart). More specifically, we wanted to demonstrate that concomitant high-quality imaging of the carotid and coronary arteries was feasible during the same CT study.

## Materials and Methods

### Study Population

Our institutional review board approved this study, and informed consent was obtained for each patient or his or her representative. Patients with hyperacute stroke who were eligible for reperfusion

therapy were not considered for this study, at least until the neurologists in charge of these patients confirmed that the patients could be approached for consent without any risk of delaying treatment.

All consecutive patients with symptoms suggestive of acute ischemic stroke 45 years of age or older referred for standard-of-care emergent CT evaluation between August 1, 2006, and September 31, 2008, were considered for enrollment in this prospective study. Standard exclusion criteria for contrast-enhanced cardiac CTA were applied (previous allergic reaction to iodinated contrast, renal disease with serum creatinine level >1.5 mg/mL, heart rate >100 beats per minute, or irregular heart rate). Patients' charts were reviewed for discharge diagnoses.

### CT Imaging Protocol

Our stroke CT protocol consisted of the following 6 steps: anteroposterior and lateral scout; noncontrast brain CT; 2 perfusion CT series of the brain; CTA of the brain, neck, and heart; and postcontrast brain CT. These CT studies were performed on a 64-section multidetector CT scanner (LightSpeed VCT; GE Healthcare, Milwaukee, Wisconsin) and were performed without prior administration of beta blockers or nitroglycerin to the patients.

In the fifth step of our CT protocol, a combined carotid coronary CTA series was performed, consisting of 2 helical acquisitions and a dual-phase contrast injection (Fig 1). The first acquisition was non-ECG gated, ascending from the aortic arch origin to the vertex of the head. The second acquisition was performed during a single breath-hold and was retrospectively ECG gated, descending from the aortic arch origin to the diaphragm. This second acquisition extended the standard-of-care stroke CT protocol coverage to include the entire heart and the full length of the coronary arteries. The acquisition parameters were as follows:  $64 \times 0.625$  mm collimation, 0.33-second gantry rotation time, 120-kV tube voltage, and 850-mA tube current. A section thickness of 1.25 mm and a pitch of 0.92 were used for the

aortic arch, and carotid and intracranial arteries, whereas a section thickness of 0.625 mm and a pitch of 0.2 were used for the coronary arteries.

The time of maximal enhancement on the perfusion CT series, considered as bolus tests, was used to calculate the contrast transit time. This contrast transit time determined the delay between initial contrast injection and the first acquisition. The dual-phase contrast injection consisted of 2 boluses of 30 cc and 60 cc iodinated contrast material (iohexol, Omnipaque; Amersham Health, Princeton, New Jersey; 350 mg/mL of iodine) injected into the right or left (preferably the right) cubital vein, followed by saline injection phases of 15 cc and 60 cc, respectively. The injection rate was 5 cc/s for both the contrast and the saline. The scanning mode for the heart was selected on the basis of the heart rate observed during a test breath-hold. One-sector reconstruction was performed if the heart rate was  $\leq 65$  beats per minute and 2-sector reconstruction, if the heart rate was  $> 65$  beats per minute. The heart rate recorded during the cardiac acquisition was later evaluated for its effect on image quality.

XYZ dose modulation was applied to all CT acquisitions except the perfusion CT series, which was performed by using 80 kV(peak) and 100 mAs.

The total amount of contrast for our complete CT protocol, including the 5 phases, was 170 cc, only 20 cc more compared with a standard stroke CT protocol without the cardiac component.

### **Carotid CTA Evaluation**

The image quality and mean attenuation of the CCAs and ICAs, aorta, and vertebral arteries were assessed by 2 neuroradiologists blinded to the patient's clinical information. The image quality of each vessel was graded on a 3-point scale (0 = excellent, 1 = good, and 2 = nondiagnostic). The percentage diagnostic was calculated by dividing the number of good or excellent vessels by the total number of assessed vessels.

The mean attenuation was measured for each vessel by placing a circular 3-mm<sup>2</sup> region of interest (200 mm<sup>2</sup> in the aorta) within each contrast-enhanced lumen. Regions of interest were also placed in the connective tissue surrounding each vessel lumen. Image noise was defined as the SD of the mean attenuation of a region of interest of 200 mm<sup>2</sup> placed in the aortic root at the level of the left main coronary artery. The CNR was then calculated by using the following equation, as proposed in previous work<sup>15,17</sup>:

$$\text{CNR} = (\text{CT Attenuation Lumen} - \text{CT Attenuation Connective Tissue}) / \text{Image Noise}.$$

CNR values were calculated in the following 12 locations: the left and right ICAs, left and right CCAs, left and right vertebral arteries, ascending aorta, descending aorta, superior vena cava, left and right internal jugular veins, and the subclavian vein contralateral to the side of contrast injection. The CNRs in the CCAs and ICAs were measured 3 cm below and 3 cm above the carotid bifurcation, respectively. The CNRs in the superior vena cava and the ascending and descending aortas were measured at the level of the right pulmonary artery. The CNRs in the internal jugular veins were measured at the level of the superior margin of the hyoid bone. The CNR in the subclavian vein was measured at the level of the sternal notch.

### **Cardiac CTA Evaluation**

To prepare the cardiac CTA for evaluation, we retrospectively reconstructed axial images of the heart by using a section thickness of 1.25 mm in 1.0-mm increments from 5% to 95% every 10% of the cardiac

cycle. Data were transferred to and postprocessed on an off-line workstation (Advantage Workstation, Version 4.4 software, GE Healthcare). Curved multiplanar reformatted images of each coronary artery were rendered and evaluated by 2 chest radiologists blinded to the patient's clinical information. The cardiac phase providing the highest quality images was selected for each artery, and the phase used was recorded.

We evaluated the image quality of the following coronary arteries: the RCA, LM, LAD, and LCX. The image quality of each coronary artery was graded on a 3-point scale (0 = excellent, 1 = good, and 2 = nondiagnostic) and involved 3 analyses: First, we performed a segment-level analysis on the basis of the 10-segment coronary tree illustrated in On-line Fig 1. We gave each coronary artery segment an image-quality score, and if nondiagnostic, we applied 1 of the following categories: poor contrast enhancement, motion artifacts, streak artifacts, tiny vessel size, heavy calcification, or pacemaker artifacts. "Motion artifacts" were defined as any blurring of the normally sharply defined vessel contour.<sup>15,18,19</sup> Poor contrast enhancement, motion artifacts, and streak artifacts were considered to be a direct result of our protocol, whereas tiny vessel size, heavy calcification, and pacemaker artifacts were not.

Next, we performed a vessel-level analysis in which each coronary artery in each patient was given an overall image-quality grade. A vessel was considered excellent if the entire vessel was diagnostic, good if 1 or 2 segments were diagnostic, and nondiagnostic if no segments were diagnostic. Those segments that were nondiagnostic for reasons unrelated to our protocol (ie, tiny vessel size, heavy calcification, or pacemaker artifacts) were omitted from this analysis.<sup>16,20</sup>

Finally, a patient-level analysis was performed. Each patient was put into 1 of 3 categories on the basis of the percentage of their 10-segment coronary tree that was diagnostic. A patient's cardiac examination was considered excellent if 75%–100% of their coronary tree was diagnostic, good if 50%–74% of their coronary tree was diagnostic, and failed if 0%–49% was considered diagnostic.

The mean attenuation was measured for each coronary artery segment. A circular 2-mm<sup>2</sup> region of interest was placed in the contrast-enhanced lumens of the coronary arteries along with the connective tissue adjacent to these arteries. Image noise was defined as the SD of CT attenuation measured in the aortic root at the level of the left main coronary artery. The CNR was then calculated, by using the following equation, as proposed in previous work<sup>15,17</sup>:

$$\text{CNR} = (\text{CT Attenuation Lumen} - \text{CT Attenuation Connective Tissue}) / \text{Image Noise}.$$

CNR values were calculated in the following 13 locations: the proximal RCA, mid-RCA (distal to the acute marginal branch), distal RCA (proximal to the origin of the PDA), acute marginal branch, PDA, LM, proximal LAD, mid-LAD (distal to the first diagonal branch), proximal first diagonal branch, proximal LCX, mid-LCX (distal to first OM), distal LCX (distal to the origin of the second OM), and proximal first OM (On-line Fig 1).

The lengths of the RCA, LM, LAD, and LCX were measured by using the curved multiplanar reformatted images. These lengths were measured manually in the centerline of the vessel from the ostium to the most distal point at which the enhanced vessel lumen was still clearly visible. The length of the RCA was defined as the length of the RCA solely or in conjunction with either the PDA or the posterolateral branch if these branches originated from the RCA and were of large diameter. The length of the LCX was defined as either the length of the entire LCX or the length of the

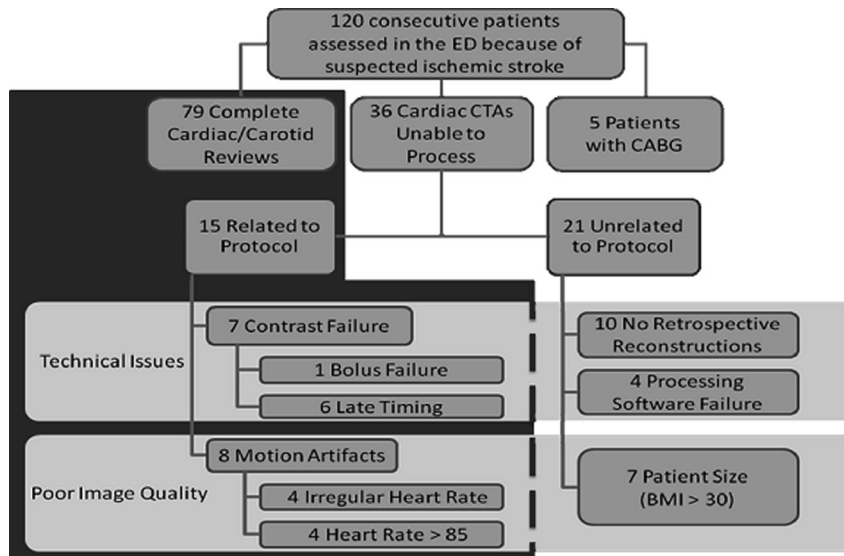


**Fig 2.** Study participants. One hundred twenty consecutive patients receiving standard-of-care stroke CT evaluation were prospectively enrolled in our study. Five patients were excluded because of CABGs. In 79 patients, both the carotid and cardiac portions of the CTA succeeded. In 36 patients, the carotid portion succeeded, but the cardiac portion failed. Fifteen of these 36 failures were directly related to our protocol, 7 were related to patient size, and 14, to technical issues. The 21 cases in which failure was unrelated to our protocol were excluded, and our image-quality analysis was performed on the remaining 94 patients.

proximal LCX plus the first or second OM if 1 of these branches had a larger diameter. In case of a left dominant circulation, the PDA was taken into account in the length of the LCX. Using the same reconstructions, we also measured the vessel lengths visualized free of motion artifacts.

### Cardiac Chamber Opacification

The cardiac chambers were evaluated for proper contrast opacification and timing. Contrast opacification was evaluated by placing regions of interest within each chamber to measure the mean attenuation level. Contrast timing was evaluated by comparing mean attenuation levels in the left cardiac chambers with those in the right cardiac chambers. We established 4 categories for timing: correct timing (greater attenuation in the left atrium/left ventricle than in the right atrium/right ventricle), early (greater attenuation in the right atrium/right ventricle than in the left atrium/left ventricle), late (low attenuation in both the left atrium/left ventricle and the right atrium/right ventricle), and bolus failure (no contrast).

### Radiation Dose for Our Protocol

Radiation dose to the patient was monitored for each study by means of the 2 standard dose indicators calculated by the CT scanner for each CT study and automatically saved to a dose report on our PACS: the  $CTDI_{vol}$  and the DLP. The  $CTDI_{vol}$  parameter is representative of the average dose delivered within the reconstructed section. The  $CTDI_{vol}$  represents the weighted CTDI divided by the pitch. The weighted CTDI describes the average dose throughout a 160 mm-diameter circular phantom made of Plexiglas (Rohm and Haas, Philadelphia, Pennsylvania) adding up the central dose weighted by a one-third factor and the peripheral dose weighted by a two-thirds factor. The DLP can be related to energy imparted to organs and can thus be used to assess overall radiation burden of a given examination. It is equal to the product of the  $CTDI_{vol}$  multiplied by the length of the scan in centimeters.<sup>21</sup> The contribution of the 2 phases of our protocol (head and neck, cardiac) to the  $CTDI_{vol}$  and the DLP was recorded.

### Statistical Analysis

Univariate and multivariate analyses involving linear regressions were conducted to assess the influence of age, weight, BMI, AP and lateral diameters of the chest, and heart rate on the percentage of coronary segments considered diagnostic; the mean CNR measured in the coronary arteries; and the proportion of diagnostic vessel lengths. Significance threshold was set at .05.

### Results

#### Patient Characteristics

Two hundred ten consecutive patients evaluated in the ED because of suspected stroke between August 1, 2006, and September 31, 2008, were considered as potential candidates for this study. Forty-three were patients with hyperacute stroke and were excluded because the consent process could have delayed the stroke reperfusion therapy for which they were eligible. Thirty-three patients were excluded because they were non-English speakers and could not give consent. Among the 134 patients who were approached to enroll in our study, 120 consented and 14 refused to enroll. In our study population of 120 patients, 79 patients had coronary arteries that could be either partially or totally assessed (Fig 2). Five patients were excluded because they had coronary artery bypass grafts. In 36 patients, the cardiac portion of the CTA failed because of technical issues ( $n = 21$ ) or poor image quality ( $n = 15$ ). Among these 36 patients, 7 failures were related to patient size and 14 were related to technical issues. The 21 cases in which failure was unrelated to our protocol were excluded, and our image-quality analysis was performed on the remaining 94 patients (79 successful cases and 15 cases in which the cardiac portion of the CTA study failed for reasons related to our protocol).

The mean age of the 94 patients (52 men, 42 women) included in our study was  $64 \pm 13$  years, with a range of 43–89 years. The mean heart rate during the cardiac portion of the CTA was  $70 \pm 13$  beats per minute, with a range of 41–102

beats per minute. The mean BMI was  $25.6 \pm 3.7$ , with a range of 16.6–36.9. The mean AP diameter of the chest was  $25.9 \pm 2.9$  cm, with a range of 19.2–35.1 cm. The mean lateral diameter of the chest was  $39.5 \pm 5.2$  cm, with a range of 28.2–50.8 cm.

The mean duration of our stroke CT protocol was  $16 \pm 3$  minutes, with a range of 11–21 minutes. The cardiac CTA portion of this protocol was responsible for  $6.5\% \pm 1.2\%$  of its total duration, with a range of 4.8%–8.8%.

Discharge diagnoses in our patient population were as follows: Thirty-six of our 94 patients (38.3%) were diagnosed with ischemic stroke at the time of their CT evaluation; the time from symptom onset in these patients until the time of their scanning was, on average,  $10.4 \pm 3.1$  hours, with a range of 5.5–15.0 hours. The use of our protocol did not delay treatment for any of our study participants. Eighteen (19.1%) were diagnosed with transient ischemic attack. Of the remaining patients, 12 (12.8%) had migraine headaches, 4 (4.3%) had aneurysms, 5 (5.3%) had brain tumors, and 19 (20.2%) had other diagnoses such as syncope, Bell palsy, and cervical radiculopathy.

### Carotid Artery Image Quality

The carotid arteries, aorta, and vertebral arteries were 100% diagnostic (rated good or excellent) in all study patients. The mean attenuation was  $>300$  HU for each artery (On-line Fig 2). The mean CNR values for the carotid arteries and the aorta were  $>10$  (On-line Table 1).

### Optimal Reconstruction Window for the Cardiac Portion of the CTA

In 68% ( $n = 54$ ) of cases, a single phase was used for the assessment of all 3 vessels—RCA, LAD, and LCX (On-line Table 2). In most of these cases (37%,  $n = 20$ ), the single phase used was 75% of the cardiac cycle (ie, the middiastolic phase); the second most-used phase (20%,  $n = 11$ ) was 45%.

### Coronary Artery Image Quality

In the segment-level analysis, a total of 931 coronary artery segments were evaluated. Of these, 163 were rated as excellent and 334, as good, amounting to 497 diagnostic segments. The following segments were nondiagnostic for reasons unrelated to our protocol: 144 segments due to tiny vessel size, 41 segments due to heavy calcification, and 2 segments due to pacemaker artifacts. The following segments were nondiagnostic for reasons related to our protocol: 169 segments due to motion artifacts, 70 segments due to poor contrast enhancement, and 8 segments due to streak artifacts. The percentage of segments considered diagnostic, excluding those segments nondiagnostic for reasons not related to our protocol, was 67% (497/744) (Fig 3A). When considering proximal segments only, the percentages that were diagnostic were as follows: 71% of the proximal RCA, 84% of the LM, 83% of the proximal LAD, and 74% of the proximal LCX. A statistically significantly higher proportion of coronary artery segments were considered diagnostic in patients with heart rates  $<85$  beats per minute than in patients with heart rates  $\geq 85$  beats per minute ( $P = .001$ ). BMI tended to influence the image quality unfavorably ( $P = .066$ ). Age, weight, and AP and lateral diameters of the chest were not found to have an important influ-

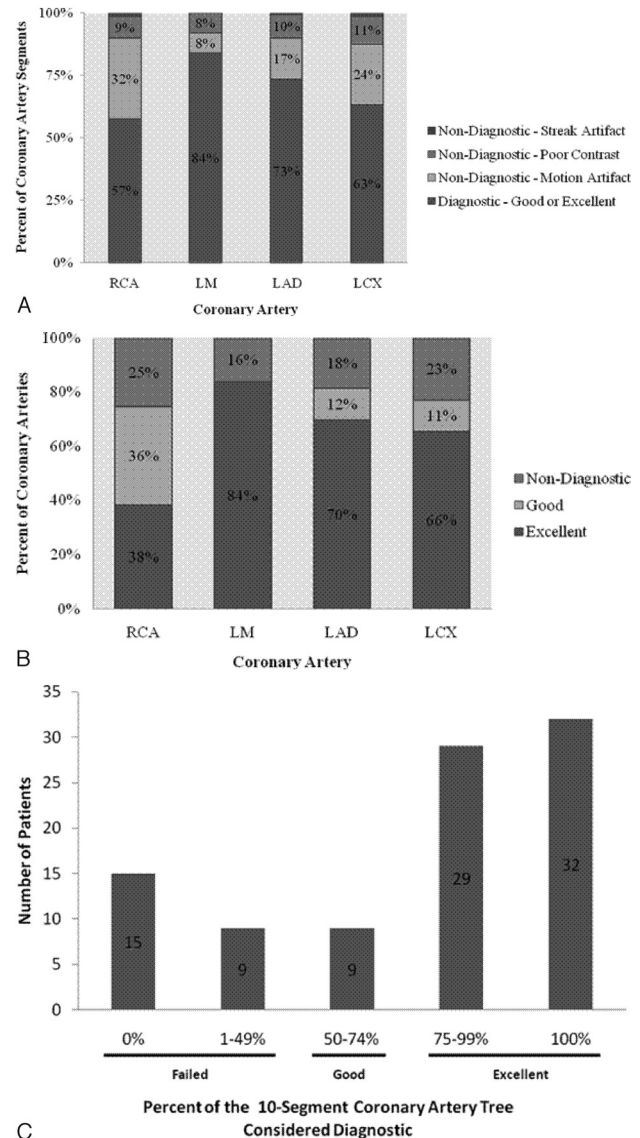


**Fig 3.** A, Segment-level analysis of coronary artery image quality. Each coronary artery segment was given an image-quality score (0 = excellent, 1 = good, and 2 = nondiagnostic). The nondiagnostic segments were separated into 3 categories: motion artifacts, poor contrast, and streak artifacts. Those segments that were nondiagnostic due to tiny vessel size, heavy calcification, or pacemaker artifacts were excluded because they were nondiagnostic for reasons not directly related to our protocol. B, Vessel-level analysis of coronary artery image quality. A coronary artery was considered excellent if the entire artery was diagnostic, good if 1 or 2 segments were diagnostic, and nondiagnostic if no segments were diagnostic. Those segments that were nondiagnostic for reasons unrelated to our protocol (ie, tiny vessel size, heavy calcification, or pacemaker artifacts) were omitted from this analysis. C, Patient-level analysis of coronary artery image quality. Cardiac examinations that were 75%–100% diagnostic were considered excellent, cardiac examinations that were 50%–74% diagnostic were considered good, and cardiac examinations that were 0%–49% diagnostic were considered failed. Most patients (65%,  $n = 61$ ) had cardiac examinations that were 75%–100% diagnostic. Nondiagnostic segments in the failed cases were primarily due to motion artifacts.

ence on coronary artery image quality. The difference in image quality between the proximal and the distal coronary artery segments was statistically significant ( $P < .001$ ).

In the vessel-level analysis, the percentages of vessels considered diagnostic (excellent or good) were as follows: the RCA, 75%; LM, 84%; LAD, 82%; and LCX, 77% (Fig 3B). In the patient-level analysis, most patients ( $n = 61$ , 65%) had excellent findings on cardiac examinations (Fig 3C).

### Coronary Artery CNR

The mean CNR in all measured coronary artery segments was  $11.7 \pm 3.9$  (On-line Table 1). The average mean attenuation for each coronary artery was  $>300$  HU (On-line Fig 3). BMI, weight, and lateral diameter of the chest significantly influenced CNR values ( $P = .026$ ,  $P = .011$ , and  $P = .003$ , respectively). CNRs tended to decrease with the AP diameter of the chest ( $P = .095$ ). In contrast, age and heart rate did not influence CNRs ( $P = .112$ , and  $P = .432$ , respectively). In a multivariate analysis involving BMI, weight, AP and lateral diameters of the chest, lateral diameter of the chest was found to be the variable with the greatest influence on CNR ( $P = 0.033$ ).

### Coronary Artery Vessel Lengths

The mean visualized lengths of the coronary arteries were as follows: RCA,  $94.5 \pm 54.1$  mm; LM,  $10.2 \pm 6.2$  mm; LAD,  $78.1 \pm 42.7$  mm; and LCX,  $48.7 \pm 32.6$  mm. On average, 68% of coronary vessel lengths were diagnostic. The percentage of vessel lengths considered diagnostic for the individual coronary arteries was as follows: 60% of the RCA, 79% of the LM, 67% of the LAD, and 65% of the LCX. A statistically significantly higher proportion of diagnostic vessel lengths was seen in patients with heart rates  $<85$  beats per minute than in those with heart rates  $\geq 85$  beats per minute ( $P = .001$ ). BMI was also found to affect diagnostic vessel lengths ( $P = .051$ ). In contrast, age, weight, and AP and lateral diameters of the chest were not significant factors influencing diagnostic vessel lengths.

### Cardiac Chambers Contrast Opacification

The average mean attenuation was greater in the left cardiac chambers than in the right (On-line Fig 4).

### Radiation Dose for Our Protocol

The mean  $CTDI_{vol}$  and DLP for the first phase of our protocol (head and neck) were the following:  $17.4 \pm 3.0$  mGy and  $726.4 \pm 41.5$  mGy\*cm, respectively. The mean  $CTDI_{vol}$  and DLP for the second phase of our protocol (cardiac) were  $75.1 \pm 8.7$  mGy and  $374.7 \pm 28.9$  mGy\*cm, respectively, and represented an increase of 45% compared with the first phase of the protocol.

### Discussion

In this study, we showed that our comprehensive stroke CT protocol, which includes the intracranial and cervical arteries, aortic arch, cardiac chambers and walls, and coronary arteries, is of adequate image quality despite use of no beta blockers. In our study group of 120 consecutive patients, the carotid portion of our proposed stroke CT protocol was consistently successful, and the cardiac portion was successful in 84% of patients. In most cases ( $n = 61$ , 65%), the patient's coronary tree was 75%–100% diagnostic; and overall, 68% of the coronary vessel lengths were diagnostic. We did not include patients with hyperacute stroke in our study because we did not want to risk delay in their treatment. However, the cardiac CTA portion of our stroke CT protocol did not significantly lengthen the duration of the stroke CT study in our patient population. Therefore, our triple rule-out stroke CT protocol has the potential to be applied in the hyperacute setting without delaying treatment.

The primary cause of coronary artery diagnostic failure related to our protocol was motion artifacts. Heart rates  $\geq 85$  beats per minute significantly increased the rate of failed cardiac/coronary studies. We could not use beta blockers to lower heart rate in our patients with a suspicion of acute ischemic stroke, in whom a slightly elevated blood pressure needs to be maintained to preserve the cerebral perfusion pressure.<sup>22</sup> Thirty-seven percent of our patients had heart rates  $\geq 85$  beats per minute. Despite this, in the vessel-level analysis, the success rate for each coronary vessel was as follows: RCA, 75%; LM, 84%; LAD, 82%; and LCX, 77%.

The proximal coronary artery image quality was significantly greater than the distal coronary artery image quality. This finding is important because visualization of the proximal portions is most clinically valuable. Patients with significant left main coronary artery disease show improved outcome with surgery rather than medical treatment,<sup>23–25</sup> along with patients with significant disease in the proximal LAD and the proximal LCX.<sup>26–28</sup> Our protocol could assist in this identification because we were able to capture 84% of the LM, 83% of the proximal LAD, and 74% of the proximal LCX.

Our protocol combines carotid and cardiac imaging in 1 CTA series, with the carotid acquisition first and the cardiac second. Combining the 2 acquisitions saves time and limits contrast, which is important because the patient may need further studies requiring contrast. The carotid arteries are scanned first to avoid streak artifacts caused by contrast in the jugular vein. The coronary arteries are scanned second to ensure greater contrast in the left cardiac chambers than in the right and to avoid streak artifacts caused by contrast in the right cardiac chambers. Further studies are needed to evaluate the potential of this CT protocol to replace TEE of the heart in the evaluation of patients with ischemic stroke for the presence of intracardiac clot.<sup>5</sup> Our CT protocol presents an additional advantage in that it can assess coronary artery disease; this assessment cannot be done with TEE. This advantage will need to be considered in the light of a small additional radiation dose, which is probably acceptable in the elderly population of patients with stroke.

Image-quality assessment of our proposed protocol yielded results comparable with those of other research groups. Kim et al<sup>29</sup> conducted a systematic analysis of image quality in 100 consecutive patients undergoing 64-section CT of the brain and neck for evaluation of stroke. In this study, the average mean attenuation for the proximal and distal ICAs was 330.0 and 314.0 HU, respectively, and the average mean attenuation for the proximal and distal CCAs was 276.0 and 334.9 HU, respectively. In our study, the average mean attenuation in the ICAs and CCAs was 343.4 and 336.5 HU, respectively. Therefore, we achieved comparable contrast opacification in the carotid arteries, while using a small amount of contrast material (only 30 cc). This was allowed by the optimal timing of our CTA acquisition based on the perfusion CT series used as bolus tests.

Delhaye et al<sup>20</sup> conducted a study in 133 consecutive patients with no beta blockers by using ECG gated multidetector CT imaging of the chest, evaluating the image quality of the coronary arteries. In 127 of these patients (95%), coronary arteries could be either partially or completely assessed. The 6 patients with failed examinations in this study were excluded,

primarily because of poor contrast enhancement in the coronary arteries. Their coronary artery segment-level image-quality analysis had the following results: The 10-segment coronary tree was 75% diagnostic, and the proximal segments were 93% diagnostic. In our study, patients with failed cardiac examinations due to poor contrast enhancement were included in our final analysis. Our coronary artery segment-level image-quality analysis had the following results: The 10-segment coronary tree was 67% diagnostic, and the proximal segments were 78% diagnostic.

Coronary artery segments that were heavily calcified were excluded in our image-quality analysis because our ability to evaluate the degree of stenosis in these segments was limited by the heavy calcifications, not by technical reasons related to our protocol. Patients with heavily calcified arteries are at higher risk of coronary ischemic events independent of underlying stenoses.<sup>30</sup>

## Conclusions

Our stroke CT protocol provides 1 examination for stroke evaluation on admission. With this 1 single protocol, it is possible to assess intracranial and cervical arteries, the aortic arch, the cardiac chambers and walls, and the coronary arteries. It is quick and of adequate image quality despite use of no beta blockers.

## References

- Adams HP Jr, Bendixen BH, Kappelle LJ, et al. Classification of subtype of acute ischemic stroke: definitions for use in a multicenter clinical trial—TOAST. *Trial of Org 10172 in Acute Stroke Treatment*. *Stroke* 1993;24:35–41
- Wintermark M, Flanders AE, Velthuis B, et al. Perfusion-CT assessment of infarct core and penumbra: receiver operating characteristic curve analysis in 130 patients suspected of acute hemispheric stroke. *Stroke* 2006;37:979–85
- Easton JD, Saver JL, Albers GW, et al. Definition and evaluation of transient ischemic attack: a scientific statement for healthcare professionals from the American Heart Association/American Stroke Association Stroke Council; Council on Cardiovascular Surgery and Anesthesia; Council on Cardiovascular Radiology and Intervention; Council on Cardiovascular Nursing; and the Interdisciplinary Council on Peripheral Vascular Disease—the American Academy of Neurology affirms the value of this statement as an educational tool for neurologists. *Stroke* 2009;40:2276–93. Epub 2009 May 7
- de Bruijn SF, Agema WR, Lammers GJ, et al. Transesophageal echocardiography is superior to transthoracic echocardiography in management of patients of any age with transient ischemic attack or stroke. *Stroke* 2006;37:2531–34
- Hur J, Kim YJ, Lee HJ, et al. Cardiac computed tomographic angiography for detection of cardiac sources of embolism in stroke patients. *Stroke* 2009;40:2073–78
- Ebrahim S, Papacosta O, Whincup P, et al. Carotid plaque, intima media thickness, cardiovascular risk factors, and prevalent cardiovascular disease in men and women: the British Regional Heart Study. *Stroke* 1999;30:841–50
- Rokey R, Rolak LA, Harati Y, et al. Coronary artery disease in patients with cerebrovascular disease: a prospective study. *Ann Neurol* 1984;16:50–53
- Di Pasquale G, Andreoli A, Pinelli G, et al. Cerebral ischemia and asymptomatic

- coronary artery disease: a prospective study of 83 patients. *Stroke* 1986;17:1098–101
- Di Pasquale G, Pinelli G, Grazi P, et al. Incidence of silent myocardial ischaemia in patients with cerebral ischaemia. *Eur Heart J* 1988;9(suppl N):104–07
- Love BB, Grover-McKay M, Biller J, et al. Coronary artery disease and cardiac events with asymptomatic and symptomatic cerebrovascular disease. *Stroke* 1992;23:939–45
- Gates P, Peppard R, Kempster P, et al. Clinically unsuspected cardiac disease in patients with cerebral ischaemia. *Clin Exp Neurol* 1987;23:75–80
- Hartmann A, Rundek T, Mast H, et al. Mortality and causes of death after first ischemic stroke: the Northern Manhattan Stroke Study. *Neurology* 2001;57:2000–05
- Petty GW, Brown RD Jr, Whisnant JP, et al. Survival and recurrence after first cerebral infarction: a population-based study in Rochester, Minnesota, 1975 through 1989. *Neurology* 1998;50:208–16
- Bronnum-Hansen H, Davidsen M, Thorvaldsen P. Long-term survival and causes of death after stroke. *Stroke* 2001;32:2131–36
- Ferencik M, Nomura CH, Maurovich-Horvat P, et al. Quantitative parameters of image quality in 64-slice computed tomography angiography of the coronary arteries. *Eur J Radiol* 2006;57:373–79
- Wintersperger BJ, Nikolaou K, von Ziegler F, et al. Image quality, motion artifacts, and reconstruction timing of 64-slice coronary computed tomography angiography with 0.33-second rotation speed. *Invest Radiol* 2006;41:436–42
- Achenbach S, Ulzheimer S, Baum U, et al. Noninvasive coronary angiography by retrospectively ECG-gated multislice spiral CT. *Circulation* 2000;102:2823–28
- Herzog C, Abolmaali N, Balzer JO, et al. Heart-rate-adapted image reconstruction in multidetector-row cardiac CT: influence of physiological and technical prerequisite on image quality. *Eur Radiol* 2002;12:2670–78
- Sanz J, Rius T, Kuschner P, et al. The importance of end-systole for optimal reconstruction protocol of coronary angiography with 16-slice multidetector computed tomography. *Invest Radiol* 2005;40:155–63
- Delhay D, Remy-Jardin M, Salem R, et al. Coronary imaging quality in routine ECG-gated multidetector CT examinations of the entire thorax: preliminary experience with a 64-slice CT system in 133 patients. *Eur Radiol* 2007;17:902–10
- Hamberg LM, Rhea JT, Hunter GJ, et al. Multi-detector row CT: radiation dose characteristics. *Radiology* 2003;226:762–72
- Mattle HP, Kappeler L, Arnold M, et al. Blood pressure and vessel recanalization in the first hours after ischemic stroke. *Stroke* 2005;36:264–68
- Caracciolo EA, Davis KB, Sopko G, et al. Comparison of surgical and medical group survival in patients with left main equivalent coronary artery disease: long-term CASS experience. *Circulation* 1995;91:2335–44
- Chaitman BR, Fisher LD, Bourassa MG, et al. Effect of coronary bypass surgery on survival patterns in subsets of patients with left main coronary artery disease: report of the Collaborative Study in Coronary Artery Surgery (CASS). *Am J Cardiol* 1981;48:765–77
- Cohen MV, Gorlin R. Main left coronary artery disease: clinical experience from 1964–1974. *Circulation* 1975;52:275–85
- Chaitman BR, Davis KB, Kaiser GC, et al. The role of coronary bypass surgery for “left main equivalent” coronary disease: the Coronary Artery Surgery Study registry. *Circulation* 1986;74(5 pt 2):III17–25
- Varnauskas E. Twelve-year follow-up of survival in the randomized European Coronary Surgery Study. *N Engl J Med* 1988;319:332–37
- Chaitman BR, Ryan TJ, Kronmal RA, et al. Coronary Artery Surgery Study (CASS): comparability of 10 year survival in randomized and randomizable patients. *J Am Coll Cardiol* 1990;16:1071–78
- Kim JJ, Dillon WP, Glastonbury CM, et al. Sixty-four-section multidetector CT-angiography of carotid arteries: a systematic analysis of image quality and artifacts. *AJNR Am J Neuroradiol* 2010;31:91–99. Epub 2009 Sep 3
- Taylor AJ, Bindeman J, Feuerstein I, et al. Coronary calcium independently predicts incident premature coronary heart disease over measured cardiovascular risk factors: mean three-year outcomes in the Prospective Army Coronary Calcium (PACC) project. *J Am Coll Cardiol* 2005;46:807–14